

# X-Ray Diffraction

Nestor Viana  
Florida International University

November 11<sup>th</sup>, 2019

## 1 Introduction

Discovered in 1895 by German physicist Wilhelm Roentgen, X-rays are a highly penetrative type of electromagnetic radiation due to their short wavelength in the order of Angstroms. Observing the variations in diffraction intensity, they render extremely useful in the exploration of the atomic structure of crystalline solids such as salts and metals, their chemical composition, and other physical properties. In this experiment we incorporate the analysis of X-ray diffraction spectroscopy to determine the atomic spacing between the ions of NaCl.

## 2 Setup

We use an X-ray spectrometer in addition to a Geiger Muller tube and a counter/voltage controller.

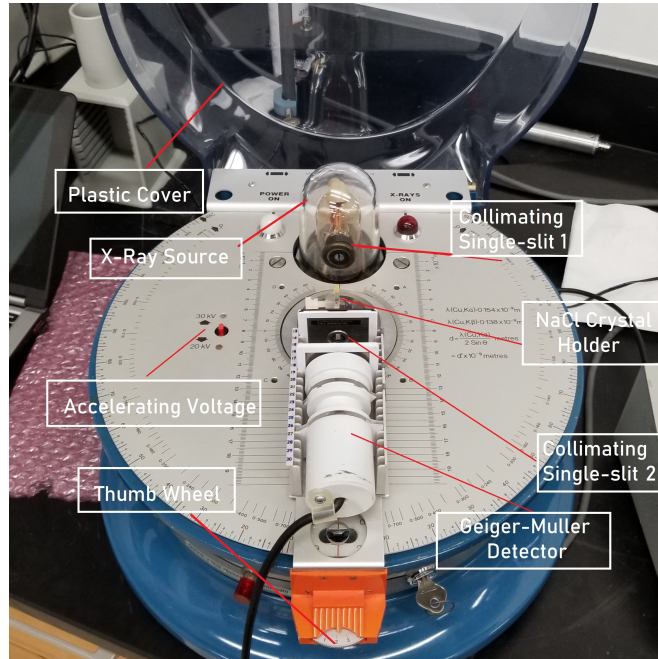


Figure 1: X-ray spectrometer.

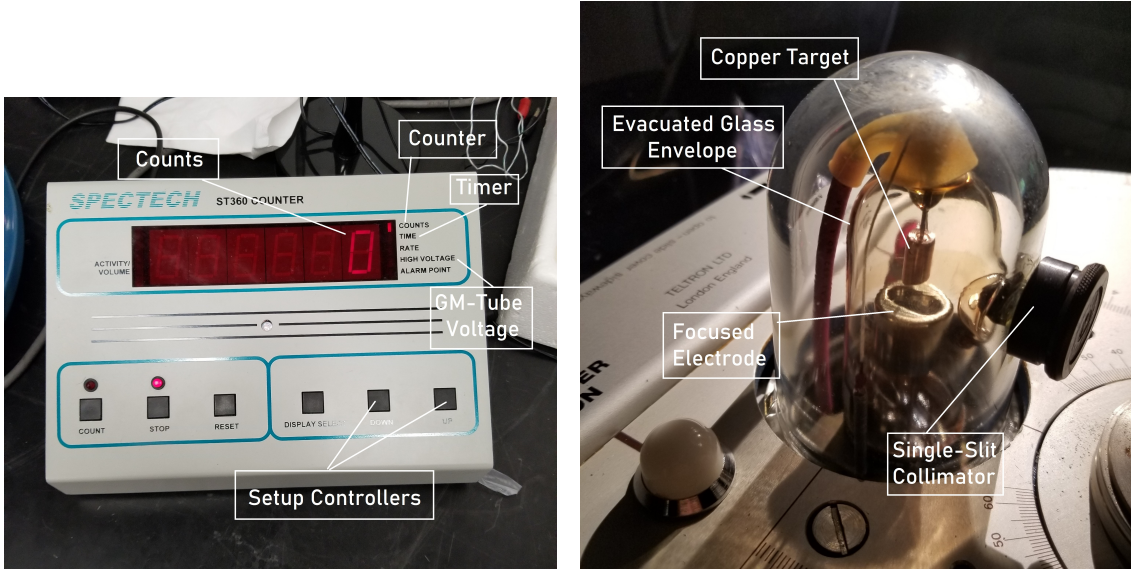


Figure 2: Counter/voltage controller and X-ray tube.

First, we place an NaCl crystal onto the crystal holder using a pair of tweezers and fix it in place. Next we set the accelerating voltage at 30 kV and close the apparatus by placing the plastic cover down. We turn on the spectrometer which creates an electric field between the focused electrode and the copper target. The temperature inside the electrode increases, heating the filament and freeing numerous amounts of electrons. Electrons are then ejected and accelerated in the presence of a strong electric field until they collide with the copper target acting as the cathode.

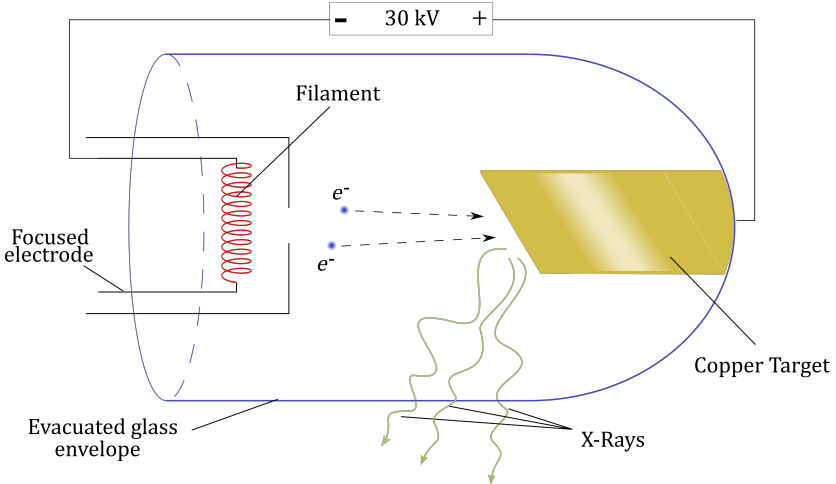


Figure 3: Inside the X-ray tube.

High speed electrons are able to collide with the inner-shell electrons of the copper nuclei (K-shell) and dislodge them from the nucleus (Figure 4 (1) and (2)). In the absence of core electrons, L- and M-shell electrons transition to the lower energy K-shell, producing short-wavelength photons. Photons released from L-K shell transitions are called  $K_{\alpha}$  X-rays (3), whereas the more energetic

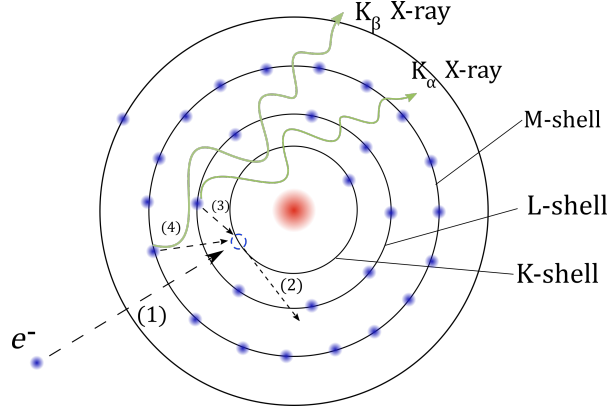


Figure 4: Collision of accelerated filament electrons with core electrons of Cu atoms.

photons produced from M-K shell transitions are known as  $K_\beta$  X-rays (4). The wavelength of each type of X-rays is predetermined by the work function of the target metal. X-rays then leave the glass envelope through a single-slit collimator which aligns them incident toward the NaCl crystal, where they reflect off the atomic planes of the crystal at angles with varying intensity. The rays finally each a second single-slit collimator that aligns them with the Geiger Muller detector.

In Figure 5, light rays (1) and (3) reach the first and second atomic planes of NaCl, respectively, with a path length difference of  $2\Delta = 2D \sin \theta$ . X-rays interfere constructively at angles  $\theta$  matching an integer multiple of the wavelength of the reflected photons  $\lambda_{K_\beta}$  and  $\lambda_{K_\alpha}$ . Such angles are characterized by a high count detected by the Geiger Muller tube set at a voltage of 420 V.

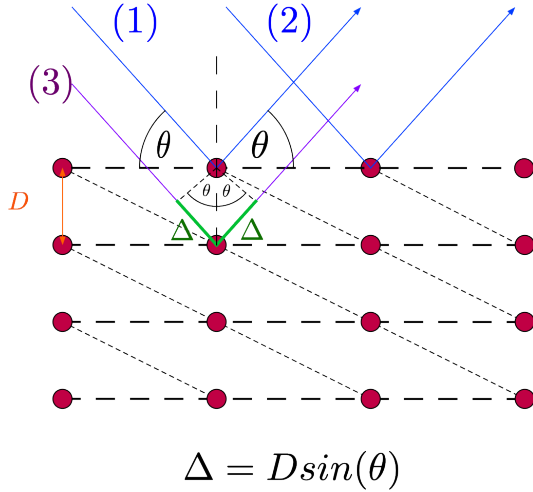


Figure 5: Reflection of X-rays incident to the atomic planes of NaCl.

That is, high counts will be detected at angles such that

$$2D \sin \theta = n\lambda \quad n = \pm 1, \pm 2, \dots \quad (1)$$

where  $n$  is the order of diffraction. This equation is known as the Bragg condition.

We take measurements of X-ray counts starting at an angle of  $2\theta = 20^\circ$  and increments of  $1^\circ$  during time intervals of 10 seconds. As we reach a count peak, we reduce the increments to  $10'$  (1/6th of a degree) using the thumb wheel shown in Figure 1.

## Theoretical Approach

A crystalline solid such as NaCl can be represented by a 3-dimensional array called a crystal lattice. Each lattice has a characteristic repetitive pattern known as a unit cell. The unit cell of NaCl consists of 4  $\text{Na}^+$  and 4  $\text{Cl}^-$  ions located at the corners of a cubic cell. From Figure 6 we can see that the volume of each unit cell is  $D^3$  and each contains half the volume of each ion.

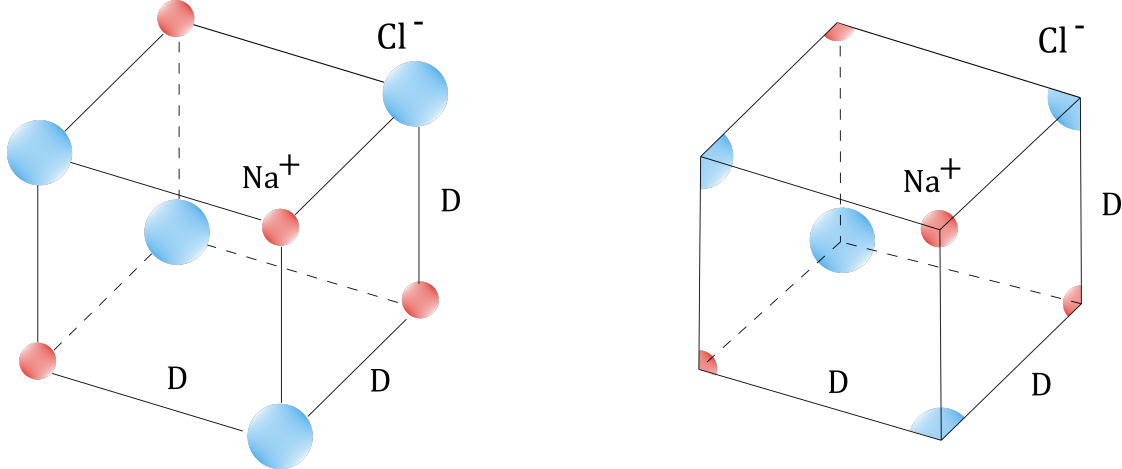


Figure 6: Unit cell of NaCl crystal lattice. Each corner contains 1/8th of an ion. Planes of parallel faces are separated by a distance  $D$ .

Therefore the mass of each unit cell is half the molar mass of NaCl. If the density of the crystal is  $\rho_0$ , then

$$\rho_0 = \frac{m}{V} = \frac{m}{D^3}$$

$$D = \sqrt[3]{\frac{m}{\rho_0}}.$$

The molar mass of NaCl is 58.44 g/mol and its density is 2.16 g/cm<sup>3</sup>. And so, we estimate the atomic spacing  $D$  to be

$$D = \sqrt[3]{\frac{(1/2)(58.44 \text{ g/mol})}{(6.02 \times 10^{23})(2.16 \text{ g/cm}^3)}} = 2.822 \text{ \AA}$$

### 3 Data

As mentioned previously, we take a total of 100 measurements (ordinary angles) for the angle of rotation  $2\theta$  of the Geiger Muller detector, starting at an angle  $2\theta = 20^\circ$ . Approaching a peak, we take as many data points (peak angles) as necessary until we are certain we have covered the range of each peak. The data is summarized in the following tables.

Detector Angles and X-ray Counts							
$2\theta$ (degrees)	Counts	$2\theta$ (degrees)	Counts	$2\theta$ (degrees)	Counts	$2\theta$ (degrees)	Counts
20	363	46	70	71	31	96	32
21	360	47	41	72	27	97	33
22	319	48	51	73	35	98	44
23	301	49	53	74	34	99	28
24	287	50	68	75	21	100	31
25	269	51	40	76	27	101	36
26	224	52	49	77	32	102	27
27	209	53	44	78	33	103	40
28	181	54	39	79	34	104	24
<b>29</b>	<b>1223</b>	55	41	80	28	105	47
30	262	56	49	81	35	106	26
31	193	57	41	82	26	107	37
<b>32</b>	<b>4205</b>	58	44	83	28	108	37
33	350	59	48	84	30	109	34
34	116	<b>60</b>	<b>162</b>	85	28	110	83
35	119	61	58	86	33	111	43
36	97	62	42	87	38	112	33
38	112	63	43	88	36	113	27
39	100	64	32	89	38	114	39
40	89	65	40	90	34	115	45
41	72	66	143	91	35	116	39
42	60	<b>67</b>	<b>339</b>	92	32	117	38
43	61	68	42	93	39	118	37
44	58	69	39	94	42	119	38
45	53	70	52	95	68	120	46

Table 1: Table of values of  $2\theta$  for ordinary angles.

Other Quantities		
Name	Variable	Value
Uncertainty in ordinary $2\theta$ angles	$\sigma_\theta$	$0.5^\circ$
Uncertainty in peak $2\theta$ angles	$\sigma_{\theta_p}$	$10'$
Wavelength of $K_\beta$ X-rays	$\lambda_{K_\beta}$	0.138 nm
Wavelength of $K_\alpha$ X-rays	$\lambda_{K_\alpha}$	0.154 nm

Table 2: Additional values required to calculate the atomic spacing  $D$ .

Angles Around Peaks and X-ray Counts							
1st Peak		2nd Peak		3rd Peak		4th Peak	
$2\theta$ (degrees)	Counts	$2\theta$ (degrees)	Counts	$2\theta$ (degrees)	Counts	$2\theta$ (degrees)	Counts
28	181	31	193	59	48	65+50'	57
28+10'	207	31+10'	256	59+10'	90	66	143
28+20'	263	31+20'	358	59+20'	165	66+10'	354
28+30'	584	31+30'	807	59+30'	202	66+20'	550
28+40'	983	31+40'	2394	59+40'	214	66+30'	583
28+50'	1261	31+50'	3694	59+50'	188	66+40'	622
29	1223	32	4205	60	162	66+50'	573
29+10'	1244	32+10'	3873	60+10'	105	67	339
29+20'	842	32+20'	3368	60+20'	67	67+10'	178
29+30'	436	32+30'	2117	60+30'	58	67+20'	111
29+40'	343	32+40'	1076			67+30'	68
29+50'	323	32+50'	555			67+40'	53
30	262	33	350				

Table 3: Peak angles: more detailed measurements around the data points highlighted in the first table.

## 4 Analysis

### 4.1 Mean and Uncertainty

#### Error in Quadratic Fit, Covariance

Dealing with counting statistics, we assign any counting measurement  $N$  the uncertainty

$$\sigma_N = \sqrt{N}. \quad (2)$$

Around each peak, we fit a second order polynomial to estimate the exact angle at which the maximum count occurs. That is, using a set of parameters  $a$ ,  $b$ , and  $c$  to fit a parabola  $y = ax^2 + bx + c$  through a set of data points, the maximum occurs at

$$\frac{dy}{dx} = 2ax + b = 0 \implies x_{\max} = -\frac{b}{2a}. \quad (3)$$

Now,  $x_{\max}$  is a function of the parameters  $a$  and  $b$ . For each count  $N_i$  there is a pair of measurements for each parameter,  $a_i$  and  $b_i$ . For the  $N$  measurements we can compute the means of the parameters,  $\bar{a}$  and  $\bar{b}$ , and so we can calculate the mean of  $x_{\max}$ ,  $\bar{x}_{\max}$ . Assuming that the errors in  $a$  and  $b$  are small, we can expand Equation 3 as

$$x_{\max,i} \approx \bar{x}_{\max} + (a_i - \bar{a}) \frac{\partial x_{\max}}{\partial a} + (b_i - \bar{b}) \frac{\partial x_{\max}}{\partial b} \quad (4)$$

where  $\bar{x}_{\max} = x_{\max}(\bar{a}, \bar{b})$ . Therefore, the variance of  $x_{\max}$  is

$$\sigma_{x_{\max}}^2 = \frac{1}{N-1} \sum_{i=1}^N (x_{\max,i} - \bar{x}_{\max})^2. \quad (5)$$

Using Equation 4, Equation 5 becomes

$$\sigma_{x_{\max}}^2 = \frac{1}{N-1} \sum_{i=1}^N \left[ (a_i - \bar{a}) \frac{\partial x_{\max}}{\partial a} + (b_i - \bar{b}) \frac{\partial x_{\max}}{\partial b} \right]^2 \quad (6)$$

Using the definition of variance on the parameters  $a$  and  $b$  we simplify the last equation to

$$\sigma_{x_{\max}}^2 = \left( \frac{\partial x_{\max}}{\partial a} \right)^2 \sigma_a^2 + \left( \frac{\partial x_{\max}}{\partial b} \right)^2 \sigma_b^2 + 2 \frac{\partial x_{\max}}{\partial a} \frac{\partial x_{\max}}{\partial b} \sigma_{ab} \quad (7)$$

Computing each partial derivative gives

$$\sigma_{x_{\max}}^2 = \frac{1}{4a^4} (b^2 \sigma_a^2 + a^2 \sigma_b^2 - 2ab \sigma_{ab}) \quad (8)$$

where we define the **covariance**  $\sigma_{ab}$  as

$$\sigma_{ab} = \frac{1}{N-1} \sum_{i=1}^N (a_i - \bar{a})(b_i - \bar{b}). \quad (9)$$

We can use Equation 9 for the propagation of uncertainties in correlated variables. The **covariance matrix** is an  $m \times m$  matrix whose entries are the covariances  $\sigma_{ij}$ ,  $i, j \in [x_1, x_2, \dots, x_m]$  of any set of  $m$  correlated variables.

## Error in Diffraction Order

Based on Figure 5, we arrived at Equation 1; namely

$$2D \sin \theta = n\lambda \quad n = \pm 1, \pm 2, \dots$$

Since there is a direct proportionality between the order  $n$  and the sine of the angle  $\theta$ , we write

$$\frac{n+1}{n} = \frac{\sin(\theta_{n+1})}{\sin(\theta_n)}. \quad (10)$$

where  $\theta_{n+1}$  the peak angle corresponding to the next diffraction order of the same type of X-rays. Rearranging this equation, we obtain

$$n = \frac{\sin(\theta_n)}{\sin(\theta_{n+1}) - \sin(\theta_n)}. \quad (11)$$

The variance of the diffraction order is then

$$\sigma_n^2 = \left( \frac{\partial n}{\partial \theta_n} \sigma_{\theta_n} \right)^2 + \left( \frac{\partial n}{\partial \theta_{n+1}} \sigma_{\theta_{n+1}} \right)^2.$$

Note that  $\sigma_{\theta_n} = \sigma_{\theta_{n+1}} = \sigma_{\theta_p}$ . Each partial derivative component yields

$$\frac{\partial n}{\partial \theta_n} = \frac{\cos(\theta_n) \sin(\theta_{n+1})}{(\sin(\theta_n) - \sin(\theta_{n+1}))^2} \quad \frac{\partial n}{\partial \theta_{n+1}} = -\frac{\sin(\theta_n) \cos(\theta_{n+1})}{(\sin(\theta_n) - \sin(\theta_{n+1}))^2}$$

leaving us with a final expression for the uncertainty in the diffraction order

$$\sigma_n = \frac{\sigma_{\theta_p}}{(\sin(\theta_n) - \sin(\theta_{n+1}))^2} \sqrt{\cos^2(\theta_n) \sin^2(\theta_{n+1}) + \sin^2(\theta_n) \cos^2(\theta_{n+1})} \quad (12)$$

## 4.2 Results

In the following graph we plot the data described in Table 1. The uncertainties are determined by Equation 2. As previously discussed,  $K_\beta$  X-rays are produced when electrons transition from the higher energy M-shell farther away from the K-shell, and so M-K shell transitions occur *less* frequently than L-K shell transitions. Therefore, the higher peaks correspond to  $K_\alpha$  X-rays and lower ones indicate  $K_\beta$  X-ray counts.

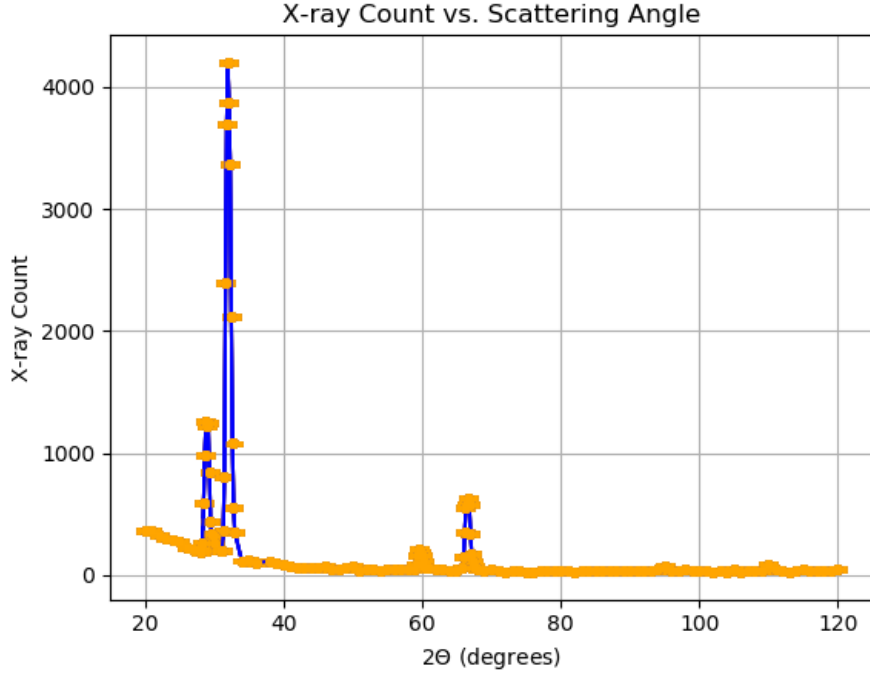


Figure 7: Plot of X-ray count and Scattering angle. Each set of peaks corresponds to different diffraction orders.

For now let us assume that the first and second sets of peaks correspond to the diffraction orders  $n = 1$  and  $n = 2$ , respectively; we will later show that this is the case. In the following graphs we select the ranges described in Table 3 and fit a quadratic polynomial  $y_i$  for each peak  $i$ ,  $i = 1, 2, 3, 4$ .

$$y_i = a_i(2\theta)^2 + b_i(2\theta) + c_i$$

Note that the fits are set on the variable  $2\theta$ , as the horizontal axis in Figure 7 depicts. The maximum of each peak occurs at

$$\frac{dy_i}{d\theta} = 8a_i\theta + 2b_i = 0 \implies \theta_{\max} = -\frac{b_i}{4a_i}. \quad (13)$$

Since the fit parameters are correlated, the variance in  $\theta_{\max}$  is obtained according to Equation 7, where the covariance(s) are provided by the covariance matrix simultaneously calculated with the parameters.

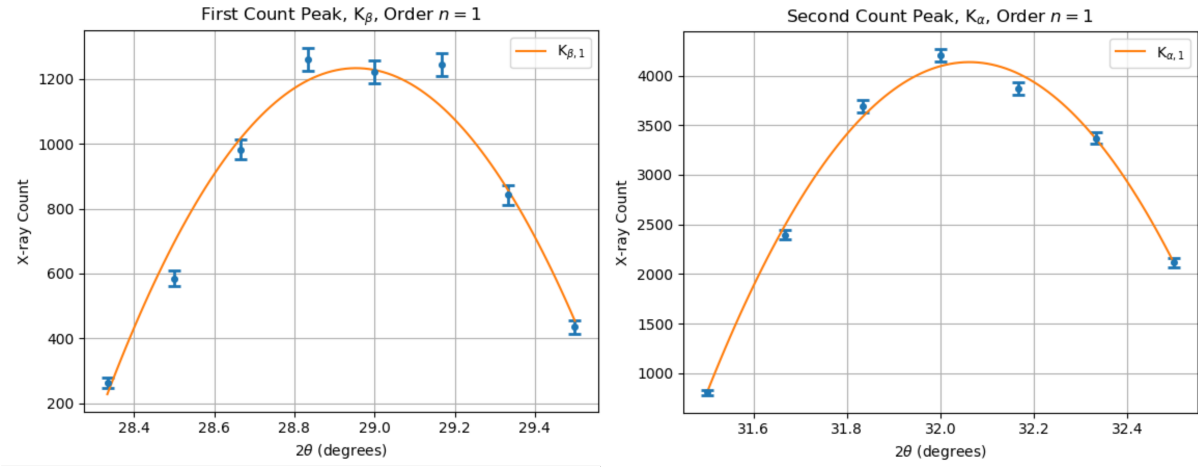


Figure 8: Quadratic fits of first order  $K_\beta$  and  $K_\alpha$  X-rays.

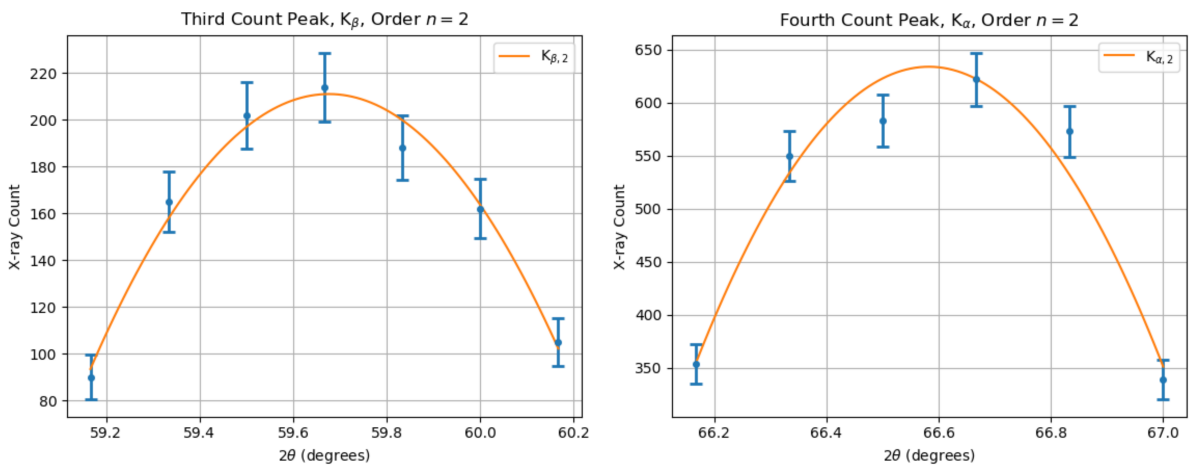


Figure 9: Quadratic fits of second order  $K_\beta$  and  $K_\alpha$  X-rays.

In the following tables we list the values of the regression parameters and their covariance matrices.

Peak #1, $K_{\beta 1}$		
Parameter	Value	Error
$a_1$	-2612.8533	69.08919
$b_1$	151303.9197	3993.29463
$c_1$	-2189176.1075	57688.78709

Peak #2, $K_{\alpha 1}$		
Parameter	Value	Error
$a_2$	-10573.2976	186.22807
$b_2$	677997.9320	11906.35944
$c_2$	-10864781.8097	190279.99527

Peak #3, $K_{\beta 2}$		
Parameter	Value	Error
$a_3$	-452.5329	45.67874
$b_3$	54011.0007	5450.37843
$c_3$	-1611377.8197	162578.83724

Peak #4, $K_{\alpha 2}$		
Parameter	Value	Error
$a_4$	-1621.2193	123.96850
$b_4$	215889.9344	16509.02844
$c_4$	-7186620.5431	549620.98688

$$\text{Cov}(K_{\beta 1}) = \begin{bmatrix} 3.328e9 & -2.303e8 & 3.985e6 \\ -2.303e8 & 1.594e7 & -2.759e5 \\ 3.985e6 & -2.759e5 & 4.773e3 \end{bmatrix}$$

$$\text{Cov}(K_{\alpha 1}) = \begin{bmatrix} 3.621e10 & -2.265e9 & 3.543e7 \\ -2.265e9 & 1.594e7 & -2.217e6 \\ 3.543e7 & -2.217e6 & 3.468e4 \end{bmatrix}$$

$$\text{Cov}(K_{\beta 2}) = \begin{bmatrix} 2.643e10 & -8.8603e8 & 7.426e6 \\ -8.8603e8 & 2.970e7 & -2.489e5 \\ 7.4265e6 & -2.489e5 & 2.086e3 \end{bmatrix}$$

$$\text{Cov}(K_{\alpha 2}) = \begin{bmatrix} 3.022e11 & -9.079e9 & 6.817e7 \\ -9.079e9 & 2.727e8 & -2.047e6 \\ 6.817e7 & -2.047e6 & 1.537e4 \end{bmatrix}$$

Using Equations 13 and 7 and the data above we calculate the following

Angles of Maxima (degrees)	Uncertainty in Maximum Angles (degrees)
$\theta_{\beta 1} = 14.47$	$\sigma_{\theta_{\beta 1}} = 0.00201$
$\theta_{\alpha 1} = 16.03$	$\sigma_{\theta_{\alpha 1}} = 0.00138$
$\theta_{\beta 2} = 29.84$	$\sigma_{\theta_{\beta 2}} = 0.00675$
$\theta_{\alpha 2} = 33.29$	$\sigma_{\theta_{\alpha 2}} = 0.00437$

Table 4: Final results for peak angles and their errors.

Now let us confirm the order of the peaks using Equation 11 and Table 4.

$$n_{\beta} = \frac{\sin(\theta_{\beta 1})}{\sin(\theta_{\beta 2}) - \sin(\theta_{\beta 1})} = \frac{\sin(14.47^\circ)}{\sin(29.84^\circ) - \sin(14.47^\circ)} = 1.0087$$

and similarly

$$n_{\alpha} = \frac{\sin(\theta_{\alpha 1})}{\sin(\theta_{\alpha 2}) - \sin(\theta_{\alpha 1})} = \frac{\sin(16.03^\circ)}{\sin(33.29^\circ) - \sin(16.03^\circ)} = 1.0125.$$

Since each pair of X-ray counts is successive, the order of first peaks is 1 and the order of the second peaks is two, as we assumed initially.

Now let us turn back to the purpose of this experiment. According to Equation 1, plotting the diffraction order  $n$  against the  $\sin \theta_{\text{peaks}}$  should return a slope equal to  $2D/\lambda$ , where  $\lambda$  is the wavelength of the  $K_\beta$  and  $K_\alpha$  X-rays and  $D$  is the desired atomic spacing of NaCl. As evidenced in the last calculations above, the diffraction order also has an uncertainty  $\sigma_n$  which we compute using equation 12. The current accepted value of the atomic spacing of NaCl is

$$D^* = 2.822 \text{ \AA}.$$

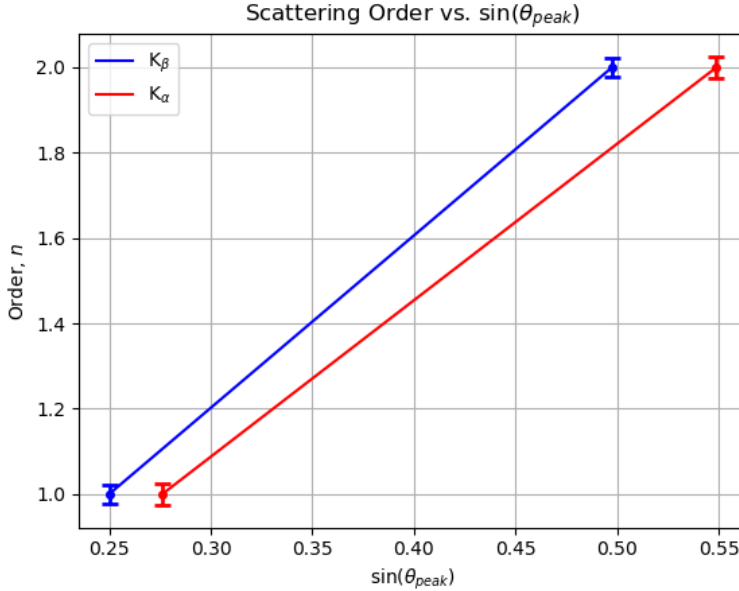


Figure 10: Diffraction order vs.  $\sin(\theta)$ .

Linear regressions of these data returns the slopes

$$m_\beta = 4.039 \pm 0.0098 \quad \text{and} \quad m_\alpha = 3.666 \pm 0.0125$$

and so we obtain

$$D_\beta = \frac{m_\beta \lambda_{K_\beta}}{2} = \frac{(4.039)(0.138 \text{ nm})}{2} = (2.787 \pm 0.012) \text{ \AA}$$

and

$$D_\alpha = \frac{m_\alpha \lambda_{K_\alpha}}{2} = \frac{(3.666)(0.154 \text{ nm})}{2} = (2.823 \pm 0.009) \text{ \AA}.$$

A simple average of these values yields the final result

$$\bar{D} = (2.805 \pm 0.011) \text{ \AA}$$

## 5 Conclusion

Our estimated value for the atomic spacing between the NaCl crystal lattice is  $(2.805 \pm 0.011)$  Å, 1.55 standard deviations away from the accepted value, 2.822 Å. Evidently, the  $K_{\alpha}$  peaks gave us more accurate results for  $D$ , 0.11 standard deviations from the published value. This was likely due to overall sharper peaks around the diffraction angles, setting more precise vertices for the parameters of the polynomial regressions. Sources of error may have come from the presence of amorphous regions on the surface of the crystal which offset the centers of the diffraction peaks. Another possible instrumental error was a polychromatic source of X-rays. As the rays left the first single-slit collimator, they encounter atmospheric gases and collide inelastically with molecules which alters their wavelength. Additionally, the thumb wheel was somewhat difficult to manipulate, thus introducing systematic error to our measurements.